


RESEARCH

Open Access



# Residual energy maximization for NOMA-enabled UAV-assisted data collection network: trajectory optimization and resource allocation

Yu Du<sup>1\*</sup> , Yijun Guo<sup>2</sup>, Jianjun Hao<sup>2</sup> and Hao Zhu<sup>2</sup>

\*Correspondence:  
duyu@bncu.edu.cn

<sup>1</sup> Business School, Beijing Language and Culture University, No. 15 Xueyuan Road, Haidian District, Beijing 100083, China

<sup>2</sup> Beijing Key Laboratory of Network System Architecture and Convergence, Beijing University of Posts and Telecommunications, No. 10 Xitucheng Road, Haidian District, Beijing 100876, China

## Abstract

In this paper, we concentrate on a non-orthogonal multiple access (NOMA)-enabled UAV data collection network for Internet of Things devices (IoT devices), where an unmanned aerial vehicle (UAV) is deployed as an aerial base station. During its flight period, the UAV can collect data from IoT devices and take advantage of the simultaneous wireless information and power transfer technology to charge the batteries of IoT devices. With the aid of NOMA, spectrum efficiency has been improved. We aim to prolong the lifetime of the IoT network, via jointly optimizing the UAV trajectory, the time allocation for information communication and wireless power transfer, the IoT devices' transmit power, as well as the IoT devices' group scheduling for NOMA. Then, we use the block coordinate descent and successive convex approximation techniques to tackle the non-convexity of the formulated problem. Numerical results show that the proposed solution increases the residual energy of the IoT devices, thus prolonging the lifetime of the network.

**Keywords:** UAV-assisted data collection, Energy maximization, Trajectory optimization, Resource allocation

## 1 Introduction

As an emerging technology, the Internet of Things (IoT) is expected to offer promising solutions to transform the operation and role of many existing industrial systems such as transportation systems and manufacturing systems [1]. As the basis of IoT applications, data collection has always been one of the most important issues for IoT to resolve for the following reasons. First, the conventional way of data collection relies heavily on ground infrastructures which cost relatively high; second, with limited energy, IoT devices (IoT devices) can hardly adapt to long-term work and third, under the condition of large number of IoT devices, the conventional orthogonal multiple access (OMA) may result in low spectrum efficiency because of the limited communication resources.

Recently, unmanned aerial vehicle (UAV) has raised great attention and been widely used in IoT due to its high possibilities of line-of-sight (LoS) air-to-ground communication

links and fully controllable mobility. However, the lifetime of IoT is usually limited by the energy availability of IoTDs. In this case, simultaneous wireless information and power transfer (SWIPT) is proposed and plays a key role in IoTDs with limited energy, since it takes full advantages of radio signals to achieve both information-transmitting and energy-transferring simultaneously [2]. Thus, many scholars introduce SWIPT into UAV-enabled IoT networks to improve the IoT lifetime. In [3], the authors utilize the UAV as a mobile data collector for sensor nodes to prolong the network lifetime, and the maximum energy consumption of all sensor nodes is minimized. In [4], the authors concentrate on leveraging UAVs to realize energy-transferring and information-transmitting simultaneously in the IoT. The power allocation and trajectory optimization problem for UAV-enabled SWIPT in IoT is investigated.

However, in the above works, in the case of a large number of IoTDs and a wide range of services, the low spectrum efficiency problem still needs to be resolved.

In another aspect, the non-orthogonal multiple access (NOMA) technique is proposed as a promising technology to improve spectrum efficiency and support massive access [5]. NOMA allows multiple users reuse the same resource block to superpose their signals in the power domain, and take advantage of successive interference cancellation (SIC) technology to decode the signal. Many works try to introduce NOMA into UAV-assisted communication systems to improve the spectrum efficiency of the wireless communication between UAV and IoTDs. In particular, in [6], all the users are served at the same time with different allocated power levels. In [7], the authors divide all IoTDs into two groups and allow two IoTDs from different groups to be served at the same channel using NOMA. IoTDs at different channels are served with OMA. However, the prior work has not taken into account the limited energy problem of IoTDs and the short lifetime problem of the IoT network. The above works show the potential advantage of applying NOMA in UAV-assisted data collection networks, where a large number of IoTDs have the need for data collection.

In this paper, we study a UAV-enabled IoT network where a UAV is deployed to use SWIPT technology to collect data from IoTDs and charge the batteries of all IoTDs to improve the residual energy of them with the aim of prolonging the IoT network lifetime. Considering that large number of IoTDs and large range of services may lead to the low spectrum efficiency of the wireless communication between UAV and IoTDs, we introduce NOMA into the IoT network and serve multiple IoTDs with the same resource block in the power domain. We aim to maximize the minimum residual energy of IoTDs, via jointly optimizing UAV trajectory, transmit power, time scheduling and NOMA group scheduling. To tackle the non-convexity of the formulated problem, we propose a suboptimal solution by utilizing the block coordinate descent (BCD) and successive convex approximation (SCA) techniques. Numerical results show that our scheme can critically improve the residual energy of IoTDs compared with the benchmark scheme.

The rest of this paper is organized as follows: Sect. 2 presents the system model and problem formulation. Section 3 describes the proposed optimization algorithm, while numerical results are discussed in Sect. 4. Section 5 provides conclusions.

## 2 Methods

### 2.1 General form of the UAV trajectory planning problem

The main research content of UAV trajectory planning is to optimize the trajectory of the UAV from the start point to the end point in a given task scenario by taking advantages of its high mobility and combining some strategies, such as resource allocation and user scheduling, while meeting the hardware limitations of the UAV and the actual task scenario constraints, so as to obtain the optimal system performance.

Therefore, the UAV trajectory planning problem can be modeled as an optimization problem under multiple constraints. Through mathematical modeling of optimization objectives, decision variables and actual scenario constraints, we can obtain the optimal UAV trajectory and other strategies by solving the optimization problem. We denote  $\mathbf{u}(t)$  as the trajectory variable and  $\mathbf{o}(t)$  as the other decision variables within the entire flight time  $t \in [0, T]$ . The UAV trajectory planning problem can be represented by a mathematical model as follows:

$$\min_{\mathbf{u}(t), \mathbf{o}(t)} f(\mathbf{u}(t), \mathbf{o}(t)) \quad (1a)$$

$$\text{s.t. } f_i(\mathbf{u}(t)) \geq 0, i = 1, 2, 3, \dots, m, \quad (1b)$$

$$g_i(\mathbf{o}(t)) \geq 0, i = 1, 2, 3, \dots, m, \quad (1c)$$

$$h_i(\mathbf{u}(t), \mathbf{o}(t)) \geq 0, i = 1, 2, 3, \dots, m. \quad (1d)$$

where  $f(\mathbf{u}(t), \mathbf{o}(t))$  represents the objective function to be optimized. It is usually an indicator function that reflects the communication performance of the system, such as throughput, system energy efficiency, etc., or some UAV indicators that need to be optimized, such as task completion time, energy consumption, etc. In addition,  $f_i(\mathbf{u}(t))$  represents constraints that only act on UAV trajectory variables,  $g_i(\mathbf{o}(t))$  represents constraints that only act on other decision variables and  $h_i(\mathbf{u}(t), \mathbf{o}(t))$  represents coupling constraints that act on both the UAV trajectory and other decision variables.

### 2.2 The UAV trajectory discretization method

In general, the variables of continuous time UAV trajectory planning problem are infinite dimensional. In order to transform this problem into an optimization problem with finite variables, it is necessary to discretize the UAV trajectory variables and other time-varying variables. The basic idea of this method is to divide the continuous trajectory variable  $\mathbf{u}(t)$  into a finite number of trajectory sequences  $\{\mathbf{u}[n]\}_{n=1}^N$ , and the UAV has a duration in each trajectory segment. At present, one of the main trajectory discretization methods is time discretization method.

When the entire flight time  $T$  of UAV is determined, the time discretization method can be used to deal with the continuous time variable. Specifically, the entire flight time  $[0, T]$  is divided into  $N$  sub-slots, and the duration of each sub-slot is  $\delta$ . In this way, the UAV trajectory variable  $\mathbf{u}(t)$ , which was originally based on continuous time representation, can be reformulated as a combination of  $N$  small line segments  $\{\mathbf{u}[n]\}_{n=1}^N$ . The distance

interval of the UAV in two consecutive time slots should satisfy the following constraint:  $\mathbf{u}[n] - \mathbf{u}[n - 1] \leq \Delta_{\max}$ , where  $\Delta_{\max}$  represents the maximum distance of the UAV in two consecutive time slots.

In order to ensure that the channel gain between the UAV and the ground communication nodes remains nearly unchanged in any time slot  $n$ ,  $\Delta_{\max}$  must meet  $\Delta_{\max} \leq H$  and  $\delta V_{\max} \leq \Delta_{\max}$ , where  $H$  and  $V_{\max}$  represent the flying altitude the maximum flying speed of the UAV, respectively. Also, the theoretical value of  $N$  must meet  $N \geq \lceil \frac{TV_{\max}}{\Delta_{\max}} \rceil$  to ensure that the velocity vector and acceleration vector of the UAV remain unchanged in the same sub-slot  $n$ .

### 2.3 Optimization algorithms of UAV trajectory planning problem

Since the UAV trajectory planning problem is usually a non-convex problem which is difficult to solve optimally, two practical algorithms have been proposed to solve this problem, namely, block coordinate descent (BCD) algorithm which is often used to solve multiple variables optimization problems and successive convex approximation (SCA) algorithm which is often used to solve non-convex problems [8].

The basic idea of BCD algorithm is to deal with multiple variables in an optimization problem in blocks, and split the original problem into multiple sub-problems of corresponding variable blocks [9]. Each time the sub-problem of one variable block is optimized, the other variable blocks remain constant. The local optimal solution of the original problem is obtained by optimizing the sub-problems alternately.

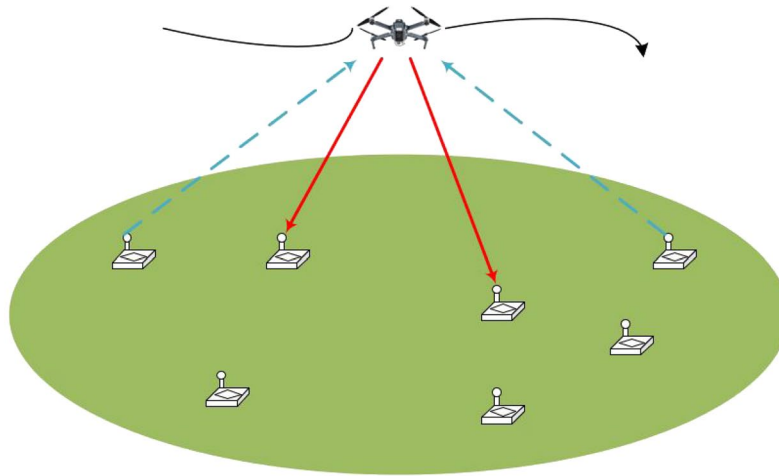
For example, we want to jointly optimize the UAV trajectory and power allocation problem, where  $\mathbf{u}[n]$  represents the trajectory sequence after time discretization of UAV trajectory variable  $\mathbf{u}(t)$ , and  $p[n]$  represents the transmission power variable after time discretization,  $h(\mathbf{u}[n], p[n])$  represents the coupling constraints of the two decision variables. It is complicated to solve this problem directly, so we first split the original problem into two independently optimized sub-problems according to the optimization variables, namely, the sub-problem of optimizing UAV trajectory and the sub-problem of optimizing power allocation. Then, fix the values of one sub-problem, solve another sub-problem to get the optimal solution and vice versa. The two sub-problems are iterated alternately until they converge to a suboptimal solution of the original problem.

The main idea of SCA technology is that for some local points given in each iteration, the non-convex target/constraint in the original problem can be approximately transformed into the corresponding convex target/constraint by using convex function property, so that an effective suboptimal solution of the original problem can be obtained by iteratively solving a series of convex problems after the approximate transformation [10]. For example, considering a simplified UAV trajectory planning problem,

$$\min_{\mathbf{u}[n]} f(\mathbf{u}[n]) \tag{2a}$$

$$\text{s.t. } f_i(\mathbf{u}[n]) \leq 0, i = 1, 2, 3, \dots, m, \tag{2b}$$

where  $\mathbf{u}[n]$  represents the UAV trajectory sequence,  $f(\mathbf{u}[n])$  represents the objective function and  $f_i(\mathbf{u}[n])$  represents a series of constraints acting on the UAV trajectory sequence. Suppose that there is a non-convex function of the optimal variable  $\mathbf{u}[n]$  in



—→ Wireless Power Transfer    - - - - -> Wireless Information Transfer

**Fig. 1** A NOMA-enabled UAV data collection scenario. Red line—wireless power transfer—the wireless power transfer period,—UAV charges the batteries of IoTds and blue line—wireless information—the wireless information transfer period,—transfer—UAV collects data from IoTds

$f_i(\mathbf{u}[n])$ , the problem is a non-convex problem which is difficult to solve. Then, we can use SCA technique to solve this problem.

Specifically, for a local point  $\mathbf{u}^{(l)}[n]$  given at the  $l$ th iteration of the optimization process, a convex upper bound of the non-convex function  $f_i(\mathbf{u}[n])$  needs to be found first,

$$f_i(\mathbf{u}[n]) \leq f_i^{\text{up}}(\mathbf{u}[n]) \tag{3}$$

We can obtain this convex upper bound by using the first-order property of concave functions, that is, the value of any concave function  $f_{\text{concave}}(y)$  is less than the value of its first-order Taylor expansion at any point,

$$f_{\text{concave}}(y) \leq f_{\text{concave}}(x) + \nabla f_{\text{concave}}(x)(y - x). \tag{4}$$

Then, we substitute the non-convex function  $f_i(\mathbf{u}[n])$  by its convex upper bound  $f_i^{\text{up}}(\mathbf{u}[n])$ , the original problem can be transformed into a new standard convex function,

$$\min_{\mathbf{u}[n]} f(\mathbf{u}[n]) \tag{5a}$$

$$\text{rms.t. } f_i^{\text{up}}(\mathbf{u}[n]) \leq 0, i = 1, 2, 3, \dots, m, \tag{5b}$$

which can be solved by existing convex optimization tools, i.e., CVX directly.

### 3 System model and problem formulation

As shown in Fig. 1, we consider a NOMA-enabled UAV data collection network where a single UAV is deployed as an aerial base station to simultaneously collect data from  $K$  IoTds, which are denoted as  $\mathcal{K} \triangleq \{1, 2, \dots, K\}$  during its flight period. We assume that the size of data that need to be collected from each IoTd is  $C$  bits.

Without loss of generality, we consider a 3D Cartesian coordinate system where the horizontal coordinate of IoTD  $k$  is fixed at  $w_k = [x_k, y_k]^T, k \in \mathcal{K}$ . The UAV trajectory needs to satisfy the following constraint:

$$\mathbf{q}[1] = \mathbf{q}[N + 1] = \mathbf{q}_I, \tag{6}$$

which implies that the UAV needs to return to its initial location by the end of each period  $T$ . We assume that the UAV flies at a constant altitude denoted as  $H$ , and its time-varying horizontal coordinate at time instant  $t \in [0, T]$  is denoted by  $\mathbf{q}(t) = [x(t), y(t)]^T$ . To make the problem more tractable, we divide the flight period  $T$  into  $N$  time slots with each time slot  $\delta = \frac{T}{N}$ . Thus, UAV trajectory can be approximated by a  $N$  two-dimensional sequence  $\mathbf{q}[n] = [x(n), y(n)]^T, n \in \mathcal{N} \triangleq \{1, 2, \dots, N\}$ . In practice, the trajectory of UAV is also subject to the maximum speed constraints

$$\|\mathbf{q}[n + 1] - \mathbf{q}[n]\|^2 \leq (V_{\max}\delta)^2, \quad \forall n \in \mathcal{N}, \tag{7}$$

where  $V_{\max}$  is the maximum speed of UAV.

During its flight period, the UAV takes advantage of SWIPT to transfer information and energy simultaneously. Each time slot with the length of  $\delta$  is divided into two period, namely, wireless power transfer (WPT) period and wireless information transfer (WIT) period. During the WPT period, UAV charges the batteries of IoTDs where the initial energy storage of IoTD  $k$  is denoted as  $E_k^{\text{init}}$ , and during the WIT period, UAV collects data from IoTDs. We assume that the proportion of time slot  $n$  which is assigned to WPT period is  $\rho[n]$ , where  $\rho[n] \in [0, 1]$ .

### 3.1 Channel model

We introduce NOMA into the network and divide IoTDs into  $M$  NOMA groups, with each group possess  $D = \frac{K}{M}$  IoTDs.<sup>1</sup> IoTDs within the same NOMA group transmit data to UAV non-orthogonally over the same frequency resource blocks (RBs). Different NOMA groups operate on different frequency RBs which are orthogonal to each other. It is assumed that the total bandwidth of system is  $W$  Hz, and each NOMA group can acquire  $F_m W_0$  Hz, where  $W_0 = \frac{W}{M}$  and  $F_m$  denote the amount of IoTDs whose channel power gain are not zero within the NOMA group  $m \in \mathcal{M} \triangleq \{1, 2, \dots, M\}$ . We define the group scheduling of group  $m$  at time slot  $n$  as  $\mathbf{g}_m[n] \triangleq \{g_{m,1}[n], \dots, g_{m,D}[n]\}$ , where  $g_{m,d}[n] \in \mathcal{K}, \forall m, n, \forall d \in \mathcal{D} \triangleq \{1, \dots, D\}$ . We assume that in each time slot, different NOMA groups cannot contain the same IoTD, and each IoTD must be served, which yields the following constraints:

$$\begin{aligned} g_{m_1, d_1}[n] &\neq g_{m_2, d_2}[n], \forall m_1, m_2, d_1, d_2, n, \\ m_1 &\neq m_2, d_1 \neq d_2. \end{aligned} \tag{8}$$

For simplicity, it is assumed that the communication links from UAV to IoTDs are dominated by LoS links, where the channel quality depends only on the UAV-IoTD distance.

<sup>1</sup> For simplicity, in this paper, we assume that  $K$  is divisible by  $M$ ; otherwise, we can add several virtual IoTDs with zero channel power gain.

Thus, the channel power gain from UAV to IoTD  $k$  at time slot  $n$  follows the free-space path loss model, which can be expressed as follows:

$$h_k[n] = \frac{\beta_0}{\|\mathbf{q}[n] - \mathbf{w}_k\|^2 + H^2}, \tag{9}$$

where  $\beta_0$  is the channel power gain at the reference distance of 1m.

In the uplink, according to SIC, the receiver first decodes the signal of IoTD whose channel power gain is stronger and treat other signals of IoTDs whose channel power gain are weaker as interference. Without loss of generality, for the UAV-IoTD channels related with group  $m$  at time slot  $n$ , we assume that  $h_{g_{m,1}[n]} \geq h_{g_{m,2}[n]} \geq \dots \geq h_{g_{m,D}[n]}$ . Thus, the achievable rate for IoTD  $k = g_{m,a}[n]$  at time slot  $n$  can be presented as [11]

$$R_k[n] = F_m W_0 \log_2 \left( 1 + \frac{P_k[n]h_k[n]}{\sum_{i=a+1}^D P_{g_{m,i}[n]}h_{g_{m,i}[n]} + N_0 d_m W_0} \right), \tag{10}$$

where  $P_k[n]$  denotes the transmit power of IoTD  $k$  at time slot  $n$ , and  $N_0$  denotes Gaussian noise power. Based on the previous settings, for each time slot  $n$  with a length of  $\delta$ , a proportion with a length of  $\rho[n]\delta$  is assigned for wireless power transfer, and the remaining period with a length of  $(1 - \rho[n])\delta$  is assigned for information transmission. Therefore, the amount of data which is collected from IoTD  $k$  by UAV is  $R_k[n](1 - \rho[n])\delta$ . To guarantee each IoTD can finish uploading all the data successfully, we must have

$$\sum_{n=1}^N R_k[n](1 - \rho[n])\delta \geq C, \quad \forall k. \tag{11}$$

### 3.2 Energy model

Based on the mentioned above, the length of the WPT period at time slot  $n$  is  $\rho[n]\delta$ , during which the UAV transfers wireless power to IoTDs and charge their batteries. The energy harvested by IoTD  $k$  at time slot  $n$  can be expressed as follows:

$$E_k^{\text{charge}}[n] = \eta P_0 h_k[n] \rho[n] \delta, \tag{12}$$

where  $\eta \in [0, 1]$  denotes the energy conversion efficiency of the receivers at IoTDs, and  $P_0$  denotes the transmit power of UAV. Thus, by the time slot  $n$ , the total energy harvested by IoTD  $k$  can be represented as follows:  $\sum_{i=1}^n E_k^{\text{charge}}[i]$ . Meanwhile, at time slot  $n$ , IoTD  $k$  needs to take a certain amount of energy to transfer information, which can be expressed as follows:  $P_k[n](1 - \rho[n])\delta$ . Thus, before the WIT period of the time slot  $n$ , the total amount of energy which IoTD  $k$  takes to transfer information is  $\sum_{i=1}^{n-1} P_k[i](1 - \rho[i])\delta$ . To ensure IoTD  $k$  has enough energy to transmit information during the remaining of time slot  $n$ , we must have

$$\begin{aligned}
 E_k^{\text{init}} + \sum_{i=1}^n E_k^{\text{charge}}[i] - \sum_{i=1}^{n-1} P_k[i](1 - \rho[i])\delta \\
 \geq P_k[n](1 - \rho[n])\delta, \quad \forall n, k.
 \end{aligned} \tag{13}$$

By the end of flight period, the residual energy of IoT D  $k$  can be written as follows:

$$E_k = E_k^{\text{init}} + \sum_{n=1}^N E_k^{\text{charge}}[n] - \sum_{n=1}^N P_k[n](1 - \rho[n])\delta. \tag{14}$$

### 3.3 Problem formulation

Our objective is to maximize the minimum residual energy of all IoT Ds, via jointly optimizing UAV trajectory, transmit power allocation of IoT DS, time scheduling and NOMA group scheduling. For notation brevity, we define transmit power allocation of IoT Ds variable set as  $\mathbf{P} = \{P_k[n], \forall k, n\}$ , time scheduling variable set as  $\rho = \{\rho[n], \forall n\}$  and NOMA group scheduling variable set as  $\mathbf{G} = \{\mathbf{g}_m[n], \forall m, n\}$ . We aim at maximizing the minimum residual energy of all IoT Ds. By defining  $\alpha = \min_k E_k$ , such an optimization problem can be formulated as follows:

$$\begin{aligned}
 (P1) : \max_{\mathbf{q}, \mathbf{P}, \rho, \mathbf{G}} \alpha \\
 \text{r.m.s.t. } E_k \geq \alpha, \quad \forall k,
 \end{aligned} \tag{15a}$$

$$0 \leq P_k[n] \leq P_{\max}, \quad \forall k, n, \tag{15b}$$

$$\begin{aligned}
 0 \leq \rho[n] \leq 1, \quad \forall n, \\
 (6), (7), (8), (11), (13),
 \end{aligned} \tag{15c}$$

where  $P_{\max}$  denotes the maximum power that IoT Ds can use to transmit information. Constraints (15b) represent the maximum IoT Ds transmit power constraint. Note that the problem (P1) is complex and non-convex due to the nonconvexity of constraints (8), (11) and (13), it is extremely difficult to be solved by utilizing existing convex optimization method.

## 4 Problem solution

Solving problem (P1) is challenging since it is a non-convex problem. In this section, we propose an iterative algorithm to solve the non-convex problem (P1) by utilizing block coordinate decent (BCD) and successive convex approximation (SCA) techniques. Specifically, we use BCD and split the optimization variables of (P1) into four blocks, denoted as  $\{\mathbf{P}, \alpha\}$ ,  $\{\rho, \alpha\}$ ,  $\{\mathbf{q}, \alpha\}$  and  $\{\mathbf{G}\}$ . Based on the previous settings, we can decompose (P1) into four sub-problems, as discussed in the following.

### 4.1 Sub-problem 1: IoT Ds transmit power optimization

For any given  $\{\mathbf{q}, \rho, \mathbf{G}\}$ , the IoT Ds transmission power allocation of problem (P1) can be optimized by solving the following problem:



$$(P2) : \max_{\mathbf{P}, \alpha} \alpha$$

s.t. (11), (13), (15b), (15a).

However, problem (P2) is still non-convex due to the non-convex constraint (6). Note that the left-hand side of constraint (6), i.e.,  $R_k[n]$  can be written as a difference of two concave functions with respect to the  $\mathbf{P}$ , i.e.,

$$R_k[n] = d_m W_0 \left[ \log_2 \left( \sum_{i=a}^d P_{g_{m,i}[n]} h_{g_{m,i}[n]} + N_0 d_m W_0 \right) - \check{R}_k[n] \right], \quad (16)$$

where  $\check{R}_k[n] = \log_2 \left( \sum_{i=a+1}^d P_{g_{m,i}[n]} h_{g_{m,i}[n]} + N_0 d_m W_0 \right)$ .

To handle the non-convex constraint (11), we apply SCA to approximate  $\check{R}_k[n]$  with a convex function in each iteration. We define  $\mathbf{P}^r \triangleq \{P_k^r[n], \forall k, \forall n\}$  as the given IoTDS transmit power in the r-th iteration. Recall that any concave function is globally upper-bounded by its first-order Taylor expansion at any point. Therefore, we have the following convex upper bound at the given point  $P_k^r[n]$

$$\begin{aligned} \check{R}_k[n] &\leq \log_2 \left( \sum_{i=a+1}^d P_{g_{m,i}[n]}^r h_{g_{m,i}[n]} + N_0 d_m W_0 \right) \\ &\quad + \sum_{i=a+1}^d F_{m,i}[n] (P_{g_{m,i}[n]} - P_{g_{m,i}[n]}^r) \triangleq \check{R}_k^{ub}[n], \end{aligned} \quad (17)$$

where  $F_{m,i}[n] = \frac{h_{g_{m,i}[n]}}{\sum_{j=a+1}^d P_{g_{m,j}[n]}^r h_{g_{m,j}[n]} + N_0 d_m W_0}$ .

With any given local point  $\mathbf{P}^r$  and (17), constraint (11) can be approximated as

$$\sum_{n=1}^N d_m W_0 \left[ \log_2 \left( \sum_{i=a}^d P_{g_{m,i}[n]} h_{g_{m,i}[n]} + N_0 d_m W_0 \right) - \check{R}_k^{ub}[n] \right] (1 - \rho[n]) \delta \geq C, \quad \forall k \quad (18)$$

, and problem (P2) can be approximated as the following problem:

$$(P3) : \max_{\mathbf{P}, \alpha} \alpha$$

s.t. (13), (15b), (15a), (18).

Problem (P3) is a convex problem, and we can solve it with existing convex optimization method.

#### 4.2 Sub-problem 2: time scheduling optimization

For any given  $\{\mathbf{q}, \mathbf{P}, \mathbf{G}\}$ , the time scheduling of problem (P2) can be optimized by solving the following problem:

$$(P4) : \max_{\rho, \alpha} \alpha$$

s.t. (13), (11), (15c), (15a).

Since problem (P4) is a standard linear programming, we can easily solve it with existing convex optimization method.

### 4.3 Sub-problem 3: UAV trajectory optimization

For any given  $\{\mathbf{P}, \rho, \mathbf{G}\}$ , the UAV trajectory of problem (P2) can be optimized by solving the following problem:

$$(P5) : \max_{\mathbf{q}, \alpha} \alpha$$

s.t. (6), (7), (11), (13), (15a).

Problem (P5) is still non-convex due to the non-convex constraints (11), (13) and (15a). As discussed in Sect. 3.1, we utilize SCA for trajectory optimization. To this end,  $R_k[n]$  in constraint (11) can be written as follows:

$$R_k[n] = d_m W_0 \left[ \hat{R}_k[n] - \log_2 \left( \sum_{i=a+1}^d \frac{P_{g_{m,i}[n]}\beta_0}{\|\mathbf{q}[n] - \mathbf{w}_{g_{m,i}[n]}\|^2 + H^2} + N_0 d_m W_0 \right) \right], \quad (19)$$

where  $\hat{R}_k[n] = \log_2 \left( \frac{P_k[n]\beta_0}{\|\mathbf{q}[n] - \mathbf{w}_k\|^2 + H^2} + \sum_{i=a+1}^d \frac{P_{g_{m,i}[n]}\beta_0}{\|\mathbf{q}[n] - \mathbf{w}_{g_{m,i}[n]}\|^2 + H^2} + N_0 d_m W_0 \right)$ .

By introducing slack variables  $\mathbf{S} \triangleq \{S_k[n] = \|\mathbf{q}[n] - \mathbf{w}_k\|^2, \forall k, \forall n\}$ , constraint (11) can be written as follows:

$$\sum_{n=1}^N d_m W_0 [\hat{R}_k[n] - \log_2 \left( \sum_{i=a+1}^d \frac{P_{g_{m,i}[n]}\beta_0}{S_{g_{m,i}[n]} + H^2} + N_0 d_m W_0 \right)] (1 - \rho[n]) \delta \geq C, \quad (20)$$

, and problem (P5) can be formulated as follows:

$$(P6) : \max_{\mathbf{q}, \alpha, \mathbf{S}} \alpha$$

s.t.  $S_k[n] \leq \|\mathbf{q}[n] - \mathbf{w}_k\|^2, \forall k, n,$  (21)  
 (6), (7), (13), (15a), (20).

To tackle the non-convexity of constraints (13), (15a), (20) and (21), we approximate them with convex functions in each iteration. We define  $\mathbf{q}^r \triangleq \{\mathbf{q}^r[n], \forall n\}$  as the given UAV trajectory in the r-th iteration. Although  $h_k[n]$  is not convex with respect to  $\mathbf{q}[n]$ , it is convex with respect to  $\|\mathbf{q}[n] - \mathbf{w}_k\|^2$ . Recall that any convex function is globally lower-bounded by its first-order Taylor expansion at any point. Therefore, we have the following convex lower bound at the given point  $\mathbf{q}^r$

$$h_k[n] \geq \frac{\beta_0}{\|\mathbf{q}^r[n] - \mathbf{w}_k\|^2 + H^2} - \frac{\beta_0(\|\mathbf{q}[n] - \mathbf{w}_k\|^2 - \|\mathbf{q}^r[n] - \mathbf{w}_k\|^2)}{(\|\mathbf{q}^r[n] - \mathbf{w}_k\|^2 + H^2)^2} \triangleq \hat{h}_k^{lb}[n]. \quad (22)$$

By substituting  $\hat{h}_k^{lb}[n]$  for  $h_k[n]$  in (13), we can approximate (13) as the following concave constraint:

$$E_k^{init} + \sum_{i=1}^n \eta P_0 \hat{h}_k^{lb}[i] \rho[i] \delta - \sum_{i=1}^{n-1} P_k[i] (1 - \rho[i]) \delta \geq P_k[n] (1 - \rho[n]) \delta, \quad \forall n, k. \quad (23)$$

Also, by substituting  $\hat{h}_k^{lb}[n]$  for  $h_k[n]$  in (15a), we can approximate (15a) as the following concave constraint

$$E_k^{init} + \sum_{n=1}^N \eta P_0 h_k^{lb}[n] \rho[n] \delta - \sum_{n=1}^N P_k[n] (1 - \rho[n]) \delta \geq \alpha, \quad \forall k. \quad (24)$$

$\hat{R}_k[n]$  in constraint (20) is convex with respect to  $\|\mathbf{q}[n] - \mathbf{w}_k\|^2$ . Therefore, we have the following convex lower bound at the given point  $\mathbf{q}^r$

$$\begin{aligned} \hat{R}_k[n] \geq & \sum_{i=a}^d A_{k,i}^r[n] (\|\mathbf{q}[n] - \mathbf{w}_{g_{m,i}[n]}\|^2 - \|\mathbf{q}^r[n] - \mathbf{w}_{g_{m,i}[n]}\|^2) \\ & + B_{k,i}^r[n] \triangleq \hat{R}_k^{lb}[n], \end{aligned} \quad (25)$$

where  $A_{k,i}^r[n]$  and  $B_{k,i}^r[n]$  are constants that are given by

$$A_{k,i}^r[n] = \frac{-\frac{P_{g_{m,i}[n]}[n] \beta_0}{(\|\mathbf{q}^r[n] - \mathbf{w}_{g_{m,i}[n]}\|^2 + H^2)^2}}{\sum_{j=a}^d \frac{P_{g_{m,i}[n]}[n] \beta_0}{(\|\mathbf{q}^r[n] - \mathbf{w}_{g_{m,i}[n]}\|^2 + H^2)} + N_0 d_m W_0}, \quad (26)$$

$$B_{k,i}^r[n] = \log_2 \left( \sum_{i=a}^d \frac{P_{g_{m,i}[n]}[n] \beta_0}{\|\mathbf{q}^r[n] - \mathbf{w}_{g_{m,i}[n]}\|^2 + H^2} + N_0 d_m W_0 \right). \quad (27)$$

By substituting  $\hat{R}_k^{lb}[n]$  for  $\hat{R}_k[n]$  in (20), we can approximate (20) as the following jointly concave constraint with respect to  $\mathbf{q}$  and  $\mathbf{S}$

$$\begin{aligned} \sum_{n=1}^N d_m W_0 [\hat{R}_k^{lb}[n] - \log_2 \left( \sum_{i=a+1}^d \frac{P_{g_{m,i}[n]}[n] \beta_0}{S_{g_{m,i}[n]}[n] + H^2} \right. \\ \left. + N_0 d_m W_0 \right)] (1 - \rho[n]) \delta \geq C. \end{aligned} \quad (28)$$

In constraint (21),  $\|\mathbf{q}[n] - \mathbf{w}_k\|^2$  is convex with respect to  $\mathbf{q}[n]$ , so constraint (21) can be approximated as

$$S_k[n] \leq \|\mathbf{q}^r[n] - \mathbf{w}_k\|^2 + 2(\mathbf{q}^r[n] - \mathbf{w}_k)^T (\mathbf{q}[n] - \mathbf{q}^r[n]), \quad \forall k, n. \quad (29)$$

Based on these, with any given local point  $\mathbf{q}^r$ , problem (P5) can be approximated as the following convex problem:

$$\begin{aligned} (P6) : \max_{\mathbf{q}, \alpha, \mathbf{S}} \alpha \\ \text{s.t. } (6), (7), (23), (24), (28), (29). \end{aligned}$$

, and problem (P6) can be solved by existing convex optimization technologies.

#### 4.4 Sub-problem 4: NOMA grouping scheduling optimization

For any given  $\{\mathbf{P}, \boldsymbol{\rho}, \mathbf{q}\}$ , the NOMA group scheduling of problem (P1) is still hard to tackle due to the non-convex nonlinear constraint (8). To make the sub-problem more

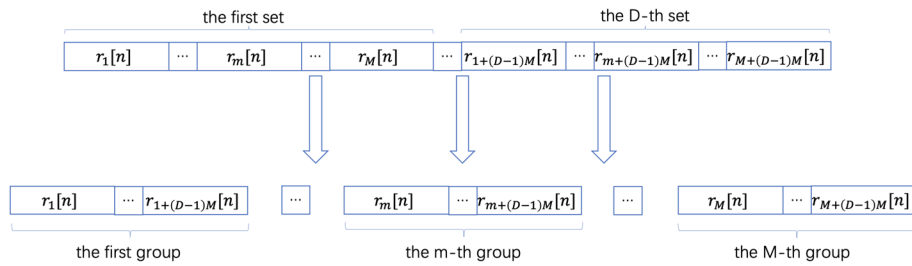


**Fig. 2** The group scheduling

tractable, we propose a heuristic algorithm for NOMA group scheduling. Considering the characteristic of NOMA, the greater the channel power gain differences between the UAV and IoTDs, the better performance of NOMA. The group scheduling we proposed aims to maximize the channel power gain differences among IoTDs in the same group. In particular, at time slot  $n$ , we first rank the channel power gain of IoTDs from large to small, and we have  $h_{r_1[n]} \geq h_{r_2[n]} \geq \dots \geq h_{r_k[n]}$ , where  $r_i[n] \in \mathcal{K}$  and  $i \in \{1, 2, \dots, k\}$ . Based on sorted results, we divide all IoTDs into  $D$  sets in order. Then, the  $m$ -th group consists of the  $m$ -th IoTD in each set, which can be presented as

$$g_{m,d}[n] = r_{m+(d-1)M}[n], \quad \forall m, d, n, \tag{30}$$

and as shown in Fig. 2.

#### 4.5 Overall algorithm

Based on the solutions to four sub-problems, an iterative algorithm for problem (P1) with BCD is proposed in Algorithm 1, which is guaranteed to converge to a sub-optimum [8].

---

**Algorithm 1** BCD Algorithm for problem P1

---

- 1: Initialize  $\mathbf{q}^0, \mathbf{P}^0, \boldsymbol{\rho}^0$  and  $\mathbf{G}^0$ . Let  $r = 0$ .
- 2: **repeat**
- 3:     Solve problem (P2.2) for given  $\{\mathbf{q}^r, \boldsymbol{\rho}^r, \mathbf{G}^r\}$  and denote the optimal solution as  $\{\mathbf{P}^{r+1}\}$ .
- 4:     Solve problem (P2.3) for given  $\{\mathbf{q}^r, \mathbf{P}^{r+1}, \mathbf{G}^r\}$  and denote the optimal solution as  $\{\boldsymbol{\rho}^{r+1}\}$ .
- 5:     Solve problem (P2.6) for given  $\{\mathbf{P}^{r+1}, \boldsymbol{\rho}^{r+1}, \mathbf{G}^r\}$ , denote the optimal solution as  $\{\mathbf{q}^{r+1}\}$ .
- 6:     Update  $\{\mathbf{G}^r\}$  as  $\{\mathbf{G}^{r+1}\}$  according to the proposed NOMA grouping scheduling.
- 7:     Update  $r = r + 1$ .
- 8: **until** The fractional increase of the objective value is below a threshold  $\varepsilon > 0$ .

---

### 5 Results and discussion

In this section, we provide numerical results to demonstrate the performance of the proposed algorithm. We distribute  $K = 12$  IoTDs in a geographical area of  $500 \times 500 \text{ m}^2$ . Other parameters are set as  $H = 50 \text{ m}$ ,  $V_{\max} = 50 \text{ m/s}$ ,  $\mathbf{q}_I = [75, 0]^T$ ,  $T = 40 \text{ s}$ ,  $W = 15 \text{ MHz}$ ,  $\beta_0 = 0 \text{ dB}$ ,  $N_0 = -120 \text{ dBm}$ ,  $D = 3$ ,  $M = 4$ ,  $C = 15 \text{ Mb}$ ,  $P_{\max} = 3 \text{ mW}$ ,  $\eta = 0.8$ ,  $P_0 = 15 \text{ W}$ .

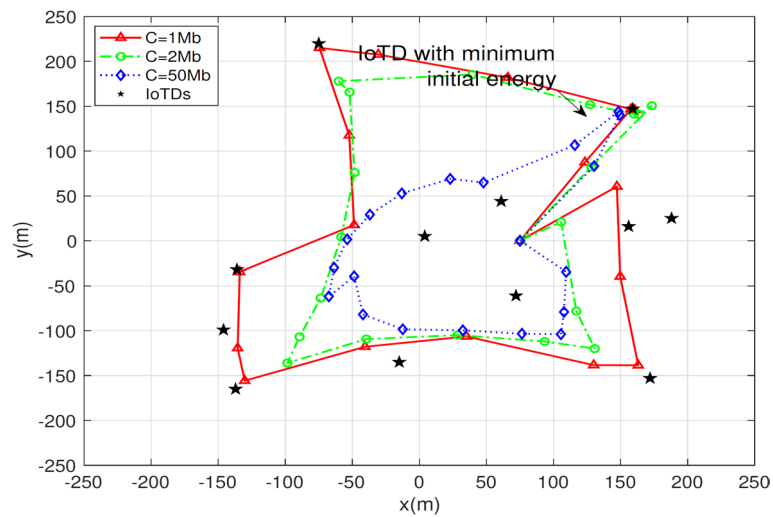


**Fig. 3** UAV trajectory under different data size  $C$ . Red line with triangle— $C = 1$  MB—the optimal UAV trajectory with  $C = 1$  MB; green line with circle— $C = 2$  MB—the optimal UAV trajectory with  $C = 2$  MB and blue line with diamond— $C = 50$  MB—the optimal UAV trajectory with  $C = 50$  MB star—IoTDs—the location of IoTDS

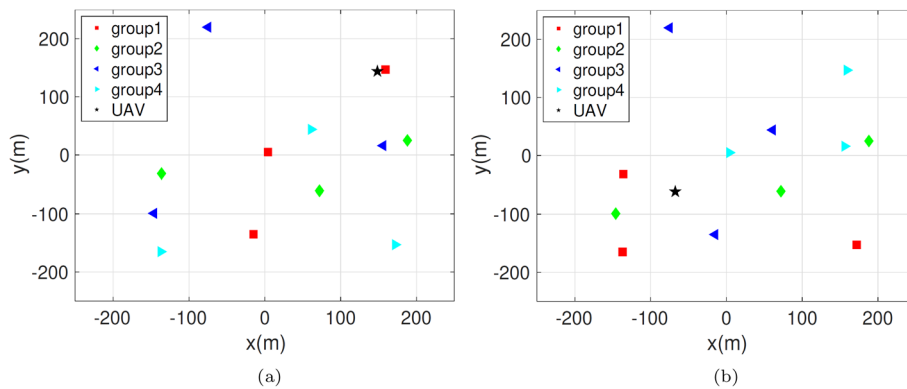


**Fig. 4** **a** NOMA grouping results at  $t = 10$ ms. **b** NOMA grouping results at  $t = 20$ ms. Square—group1—the location of IoTDS within NOMA group 1; diamond—group2—the location of IoTDS within NOMA group 2; left triangle—group3—the location of IoTDS within NOMA group 3 and right triangle—group4—the location of IoTDS within NOMA group 4 star—UAV—the location of UAV

First, we study how the amount of data which each IoT need to finish uploading affects the optimal UAV trajectory. As shown in Fig. 3, with a small  $C$ , UAV can pass through the above of every IoT to collect data and charge their batteries more efficiently. On the contrary, a large  $C$  leads to limited time, which makes UAV trajectory only cover the central area. However, we can observe that UAV always flies pass through the above of the IoT with minimum initial energy to transmit more energy to it. Figure 4a and b presents the NOMA group scheduling at two different time slots. It is observed that IoTs which are about the same distance to UAV are always grouped into different groups to increase the differences of channel power gain of IoTs among the same group.

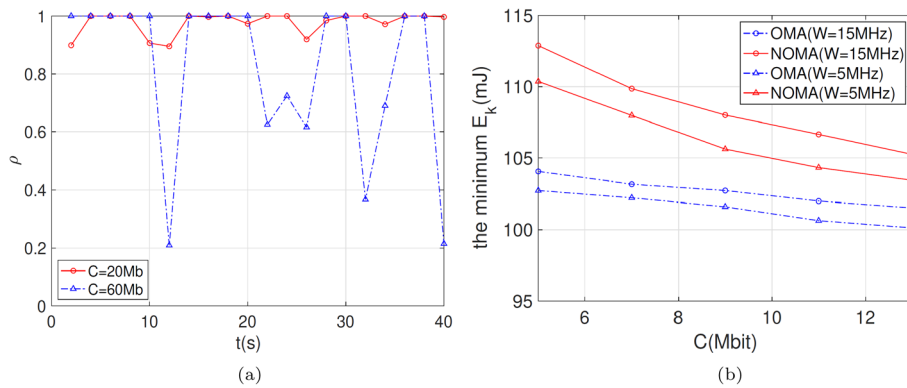


**Fig. 5** **a** Time scheduling under different  $C$ . **b** Minimum residual energy of NOMA and OMA under different bandwidth  $W$ . Red line with circle in **a**— $C = 20$  Mb—the time scheduling—under  $C = 20$  MB; blue line with triangle in **a**— $C = 60$  Mb—the time scheduling—under  $C = 60$  MB; blue line with circle in **b**—OMA ( $W = 15$  MHz)—the OMA scheduling—under  $W = 15$  MHz; red line with circle in **b**—NOMA ( $W = 15$  MHz)—the NOMA scheduling—under  $W = 15$  MHz; blue line with triangle in **b**—OMA ( $W = 5$  MHz)—the OMA scheduling—under  $W = 5$  MHz and red line with triangle in **b**—NOMA ( $W = 5$  MHz)—the NOMA scheduling—under  $W = 5$  MHz

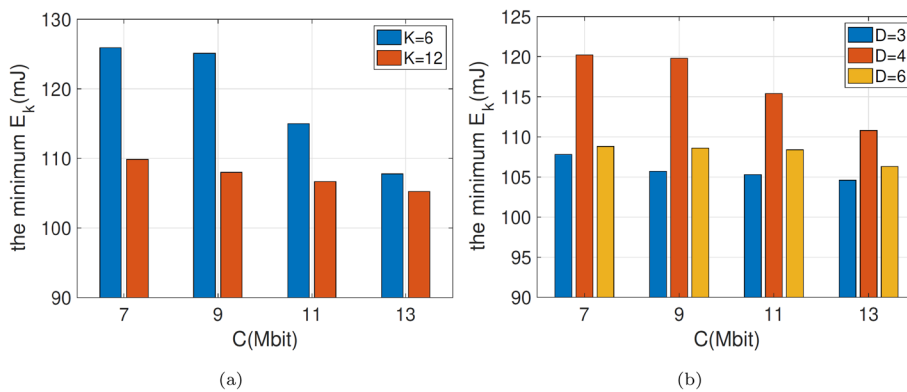


**Fig. 6** **a** Minimum residual energy of NOMA under different amounts of IoT devices  $K$ . **b** Minimum residual energy of NOMA under the different amounts of IoT devices in each group  $D$ . Blue bar in **a**  $K = 6$ —the NOMA scheduling under  $K = 6$ ; orange bar in **a**— $K = 12$ —the NOMA scheduling under  $K = 12$ ; blue bar in **b**— $D = 3$ —the NOMA scheduling under  $D = 3$ ; orange bar in **b**— $D = 4$ —the NOMA scheduling under  $D = 4$  and yellow bar in **b**— $D = 6$ —the NOMA scheduling under  $D = 6$

In Fig. 5a, the results of time scheduling strategy under different amounts of data each IoT device need to transmit, i.e.,  $C$ , are plotted. It is shown that, first, the transmission is fluctuation over the time, since the UAVs tend to transmit when flying near the IoT devices. Second, with more data for IoT devices to finish uploading, more time will be allocated for data collection, and that is to say that  $\rho$  is smaller.

Figure 5b illustrates a comparison between NOMA and orthogonal multiple access (OMA) under different bandwidth  $W$  of system. It is observed that with the increase of  $W$ , the performance of both two schemes will be improved, and the NOMA scheme that we proposed always outperforms the OMA scheme under the same condition.

Moreover, Fig. 6a presents the performance of NOMA scheme we proposed under different amounts of IoT devices  $K$ . It is easy to see with the increase of  $K$ , the performance

decreases. Figure 6b shows how the amount of IoTDs in each NOMA group, denoted as  $D$ , affects the performance of NOMA scheme. It is easily observed that the increasement of  $D$  may improve the performance as expected. However, we cannot endlessly keep increasing the value of  $D$ , which has an optimal value denoted as  $D_{\text{optimal}}$ . When  $D$  is larger than  $D_{\text{optimal}}$ , the performance will degrade instead.

## 6 Conclusion

This paper studies a new NOMA-enabled UAV data collection system for IoTDs, where the UAV is deployed to collect data from IoTDs and charge the batteries of them to prolong the lifetime of the IoT network. We formulate the residual energy maximization problem of IoTDs, via jointly optimizing UAV trajectory, transmit power allocation of IoTDs, time scheduling and NOMA group scheduling. Then, we propose an iterative algorithm to solve the formulated problem suboptimally. Numerical results show that our schemes can effectively increase the residual energy of the IoTDs, thus prolonging the lifetime of the network.

### Abbreviations

NOMA	Non-orthogonal multiple access
IoTds	Internet of Things devices
UAV	Unmanned aerial vehicle
SWIPT	Simultaneous wireless information and power transfer
BCD	Block coordinate decent
SCA	Successive convex approximation
OMA	Orthogonal multiple access
LoS	Line-of-sight
SIC	Successive interference cancelation
WPT	Wireless power transfer
WIT	Wireless information transfer
RBs	Resource blocks

### Acknowledgements

Not applicable.

### Author contributions

All authors proposed the method and helped revising the algorithm and designing the experiment. All authors read and approved the final manuscript.

### Funding

This research project is supported by Science Foundation of Beijing Language and Culture University (supported by "the Fundamental Research Funds for the Central Universities") (23YJ090011).

### Availability of data and materials

The authors confirm that the data supporting the findings of this study are available within the article.

### Declarations

#### Competing interests

The authors declare that they have no competing interests.

Received: 6 August 2023 Accepted: 7 September 2023

Published: 13 September 2023

### References

1. L. Da Xu, W. He, S. Li, Internet of things in industries: a survey. *IEEE Trans. Ind. Inf.* **10**(4), 2233–2243 (2014)
2. F. Huang, J. Chen, H. Wang, G. Ding, Y. Gong, Y. Yang, Multiple-UAV-assisted SWIPT in internet of things: user association and power allocation. *IEEE Access* **7**, 124244–124255 (2019)
3. C. Zhan, Y. Zeng, R. Zhang, Energy-efficient data collection in UAV enabled wireless sensor network. *IEEE Wireless Commun. Lett.* **7**(3), 328–331 (2018)

4. F. Huang et al., UAV-assisted SWIPT in internet of things with power splitting: trajectory design and power allocation. *IEEE Access* **7**, 124244–124255 (2019)
5. K. Higuchi, Y. Kishiyama, Non-orthogonal access with successive interference cancellation for future radio access. *IEICE Trans. Commun.* **E98B**(3), 403–414 (2015)
6. A. Farajzadeh, O. Ercetin, H. Yanikomeroglu, UAV Data collection over NOMA backscatter networks: UAV altitude and trajectory optimization, in 2019 IEEE International Conference on Communications (ICC), pp. 1–7 (2019)
7. J. Zhao, Y. Wang, Z. Fei, X. Wang, Z. Miao, NOMA-aided UAV data collection system: trajectory optimization and communication design. *IEEE Access* **8**, 155843–155858 (2020)
8. Q. Wu, Y. Zeng, R. Zhang, Joint trajectory and communication design for multi-UAV enabled wireless networks. *IEEE Trans. Wireless Commun.* **17**(3), 2109–2121 (2018)
9. G. Zhang, Q. Wu, M. Cui, R. Zhang, Securing UAV communications via joint trajectory and power control. *IEEE Trans. Wireless Commun.* **18**(2), 1376–1389 (2019)
10. M. Razaviyayn, Successive convex approximation: analysis and applications, University of Minnesota (2014)
11. W. Chen, S. Zhao, R. Zhang, L. Yang, UAV-Assisted data collection with non-orthogonal multiple access, in 2020 IEEE wireless communications and networking conference (WCNC), pp. 1–6 (2020)

### Publisher's Note

Springer Nature remains neutral with regard to jurisdictional claims in published maps and institutional affiliations.

**Submit your manuscript to a SpringerOpen<sup>®</sup> journal and benefit from:**

- ▶ Convenient online submission
- ▶ Rigorous peer review
- ▶ Open access: articles freely available online
- ▶ High visibility within the field
- ▶ Retaining the copyright to your article

---

Submit your next manuscript at ▶ [springeropen.com](https://www.springeropen.com)

---